JOURNAL OF THEORETICAL AND APPLIED MECHANICS
50, 2, pp. 531-548, Warsaw 2012
50th Anniversary of JTAM

INVESTIGATION OF AXIAL CRUSHING BEHAVIOUR OF A COMPOSITE FUSELAGE MODEL USING THE COHESIVE ELEMENTS

F. Mustapha, N.W. Sim
Universiti Putra Malaysia, Department of Aerospace Engineering, Serdang, Selangor, Malaysia
e-mail: faizal@eng.upm.edu.my; weisim1984@yahoo.com

A. Shahrjerdi
University of Malayer, Department of Mechanical Engineering, Iran
e-mail: alishahrjerdi2000@yahoo.com

Finite element analysis (FEA) on a new fabrication miniature composite fuselage structure under axial compression loading is presented. ABAQUS/Explicit simulation is employed to predict the crushing behaviour and mechanical strength from the initial compression loading to the final failure mode. A woven C-glass fiber/epoxy 200 g/m^2 composite laminated with orthotropic elastic material properties is used for the fuselage model. This proposed model is established to observe the crushing load and collapse modes under an axial compression impact. Adhesively bonded joint progression is generated using the technique of cohesive element. Various angles of the lamina are deliberated in the analysis to acquire and imagine the effect of the angle of orientation. Composite lamina angles are examined and validated using FEA modelling as a numerical parametric study. The results show that the finite element analysis using ABAQUS/Explicit can reproduce satisfactorily the load-deflection response. It can be concluded that special cases of antisymmetric lamination are found to have the strongest resistance to the applied load.

Key words: adhesively bonded joint, composite fuselage, FEA, crushing behaviour, C-glass fiber/epoxy, cohesive elements

1. Introduction

The significant drawbacks of the filament winding composite fabrication process can be described in terms of expensive equipment, time-consuming production process and inflexibility regarding the shape of the structure to be

wound (Koussios *et al.*, 2004). A novel fabrication method of a miniature composite fuselage was successfully investigated by Dahdi *et al.* (2009). In their research, they estimated the possibility of using the combining mould technique to replace the method of filament winding by integrating the woven fiber composite laminated with an adhesive butt joint. This technique can sustain an axial compression impact from debonding failure. According to the advantages of this novel fabrication technique, it can be implemented in the real aerospace world.

Recently, analytical and numerical methods have been studied by many researches to present the crushing behaviour on the composite tube and cylindrical shells. Some researchers investigated the crushing response of composite shell subjects to axial compression (Chamis and Abumeri, 2005; Vaziri, 2007). Some investigations employed ABAQUS as a numerical tool to crushing simulation and analysis. Bisagni (2005) studied dynamic buckling of thin-walled carbon fiber reinforced plastics (CFRP) shell structures under axial compression. His approach was based on the equations of motion, which were numerically solved using a finite element code (ABAQUS/Explicit). He also used numerical models that were validated by experimental static buckling tests. In another interesting research, modelling of delaminated composite cylindrical shells with a linear material and under axial compression was considered by Tafreshi (2004, 2006). Nonlinear finite element analysis using ABAQUS/Explicit was employed by Mahdi *et al.* (2001, 2006) to study the crushing behaviour of a filament-wound laminated cone-cone intersection composite shell. The validation of their research was also experimentally investigated under a uniform axial load. They considered axially crushed cotton fibre composite corrugated tubes in their researches. In another research, experimental and numerical dynamic responses with damage modelling of filament wound glass/epoxy tubes were explored by Tarfaoui *et al.* (2008). Validation of experimental crushing behaviour of a filament wound C-glass fiber/epoxy 200 g/m^2 miniature fuselage using simulation technique was executed by Yidris and Mokhtar (2007). Mamalis *et al.* (2006) studied the crushing response of square carbon FRP tubes using finite element modelling subjected to static and dynamic axial compression. Xiao *et al.* (2009) and Zarei *et al.* (2008) investigated the crushing response of braided composite tubes and thermoplastic composite crash boxes, respectively. Crushing of conical composite shells were considered also by Morthorst and Horst (2006). These research works have been verified by experimental and numerical crushing simulation using LS-DYNA.

ABAQUS /Explicit as an FEA's software is employed in this research. The reliability of ABAQUS in performing non-linear analysis on crushing has been

proven in the literature (Goyal and Johnson, 2008; Yang *et al.*, 2009; Zhang *et al.*, 2008). Furthermore, ABAQUS offers composite layups to facilitate the composite model set up. It can be added that ABAQUS allows the user to define the material properties in the modelling of the progressive damage of an adhesive bonded joint.

In this paper, an FEA model on composite cylindrical structures with an adhesively bonded butt joint under axial compression is proposed to investigate the collapse modes and to compare various angular composite laminas. There are many publications available on the buckling analysis of filament wound cylindrical shells and tubes subject to axial compression. To the authors' knowledge, no prior work has been done in the area of crushing analysis on the adhesive bonded joint in a composite cylindrical shell structure with various angles of the lamina under axial compression.

2. FEA via ABAQUS/Explicit

All physical structures are nonlinear, since a nonlinear structural problem is one in which the structure stiffness changes as it deforms. If the displacements in a model due to loading are relatively small during a step, the effects may be small enough and be ignored. However, in the cases where the loads acting on a model result in large displacements, nonlinear geometric effects can become important. A nonlinear analysis should be required to observe crushing responses from initial compression loading to final failure under geometrically nonlinear deformations. Approaches of fracture mechanics are often used for simulation of damage propagation due to high-stress gradients appearing at crack fronts. The employment of solely stress-based criteria is not useful (Balzani and Wagner, 2008). The linear Elastic Fracture Mechanics (LEFM) approach is often employed in failure of the adhesive joint, and it can only be applied when the starting crack exists and when material nonlinearities can be neglected (Wimmer *et al.*, 2006). Based on geometric and material nonlinearity, a nonlinear solver to establish equilibrium is required. It can be explained that the geometric nonlinearity is due to large rotation kinematics and large strain, while the nonlinear material behaviour is due to degradation of the adhesive material properties and the stiffness during progressive failure of the damage initiation and evolution mechanisms (Goyal and Johnson, 2008; Zhang *et al.*, 2008). An incremental-iterative approach is taken for the nonlinear finite element analysis, and the Newton-Raphson method is utilized to trace the loading path of the structure with a displacement-control analysis. During the

analysis for each load step, an additional iteration may be essential to verify whether there is another initiation of new failure events in individual elements. To obtain a converged solution maximum, the number of iterations is significant. The iteration is postponed when the routine cannot be reiterated with a smaller increment (Zhang *et al.*, 2008). ABAQUS/Explicit is a special-purpose analysis product that employs an explicit dynamic finite element formulation. This product can be used for short, transient dynamic events, such as impact and blast problems, and is also very efficient for highly nonlinear problems involving changing contact conditions. ABAQUS also offers composite layups to facilitate the composite model set up, and the cohesive element technique allows the user to define material properties in the modelling of the progressive damage of the adhesive bonded joint. It can be estimated that the results, once the simulation has been completed, and the reaction forces, displacements, energy or other fundamental variables have been extracted.

3. Modelling process and FEA methodology

An eight-layer composite orthotropic, woven C-glass fiber/epoxy 200 g/m^2 [90_8] with total thickness of 3mm is used to fabricate the fuselage structure. The fuselage dimensions are shown in Fig. 1.

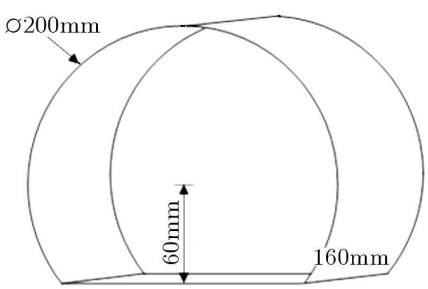

Fig. 1. Fuselage structure section

As it is shown in Fig. 2 and Fig. 3, in the geometric modelling process, the model consisted of two deformable parts for two fuselage sections, two adhesive layers, and two rigid surfaces as tools (RS1 and RS2). It can be noted that the fuselage sections are bonded with the zero thickness adhesive layers along the fuselage edge. The fuselage sections and adhesive elements are considered as deformable parts that can be deformed under applied loads. Tools are modelled as discrete rigid parts because they were much stiffer than the fuselage

section. The discrete rigid part is assumed to be unbending, and is used in contact analyses to model bodies that cannot deform. RS1 is displaced 80 mm downward at the Z-direction to crash toward the fuselage section bonded with the adhesive joint; RS2 is fixed to hold in a position during axial loading.

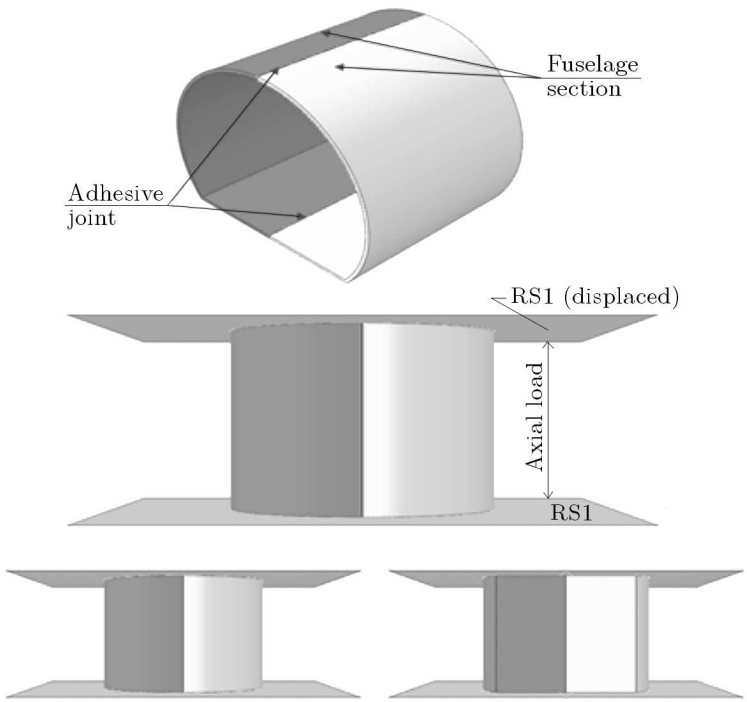

Fig. 2. Component arrangement

In the finite element modelling, mesh convergence is studied for the mesh size 3, 5, and 8 mm (Table 1). The agreement of the FEA with experimental results suggests that the mesh used is adequate to predict the overall response accurately. In the meshing process, 3 mm mesh size is employed in the fuselage modelling, because it is finer and more accurate as well as more realistic to capture the deformation modes of the structure under compression loading. Figure 4 shows the meshing model of the fuselage sections and the solid cohesive element.

For cohesive meshing elements, a 3 mm mesh size is employed in this research (Fig. 4). Swept or offset meshing techniques should be used to generate the mesh in the cohesive layer because these tools produce meshes that are oriented consistently with the stack direction that is aligned with the offset direction. The type of the cohesive element is COH3D8 for the adhesive bonded

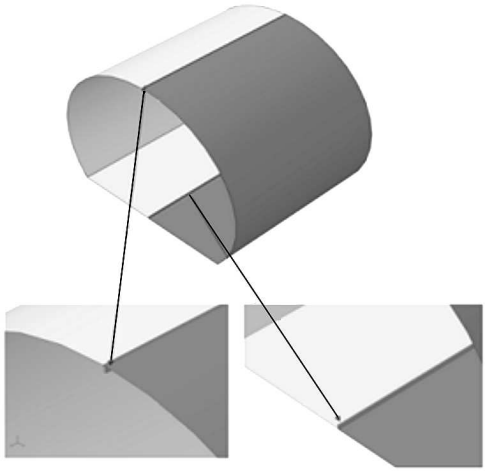

Fig. 3. Assembled adhesive parts

Table 1. Convergence study in the mesh size

Mesh size [mm]	Mesh elements	Peak load [kN]
3	11138	78
5	8316	76
8	3444	81

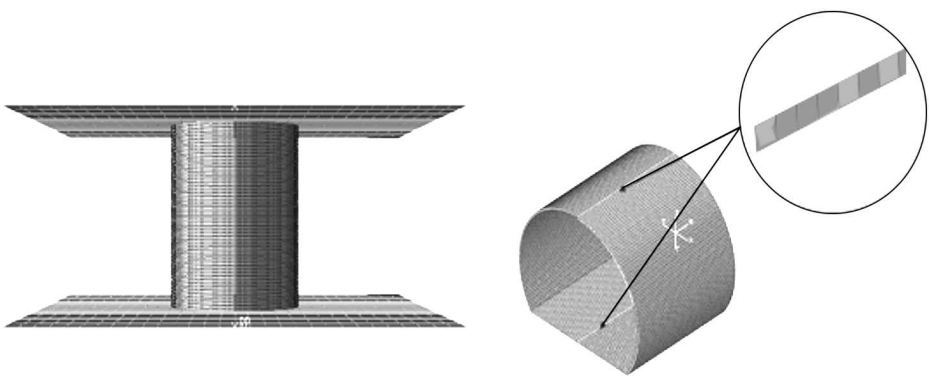

Fig. 4. Fuselage sections and solid cohesive meshing

joint in ABACOUS package. It is considerable that the thickness of the cohesive elements is defaulted to zero. The geometric region that represents the cohesive layer should be defined as a solid, even if the thickness of the layer is

close to zero. To avoid numerical problems, it is recommended to use a value of 10^{-4} or greater for the thickness of the cohesive layer in the modelling process. If the actual thickness of the layer is less than this value, the actual thickness in the initial thickness field of the cohesive section editor should be specified. The mesh size of rigid surfaces was defined approximately 10 mm for all edges of a part. The element shape was considered quadrangle and an auto-meshing technique was used to generate the meshed structure. It can be noted that the mesh distortion can be decreased by minimizing the mesh transition.

4. FEA mathematical process

In the recent years, fracture mechanics has emerged as a theory which can be used successfully in both deriving failure criteria and developing computational tools. Fracture mechanics has also been used for simulation of delamination and adhesives (Trias *et al.*, 2006). The virtual crack closure technique (VCCT) and cohesive elements are in the minds of all finite element software developers. VCCT is based on the assumption that the energy released when a crack is opened from a to $a + \Delta a$ is the same energy required to close the crack from the length $a + \Delta a$ to the length a. A typical modelization of a single lap joint that can be employed in this research is shown in Fig. 5. As it is shown there, the nodes in the adhesive region are connected through rigid links with a spring at their tip, as is performed generally.

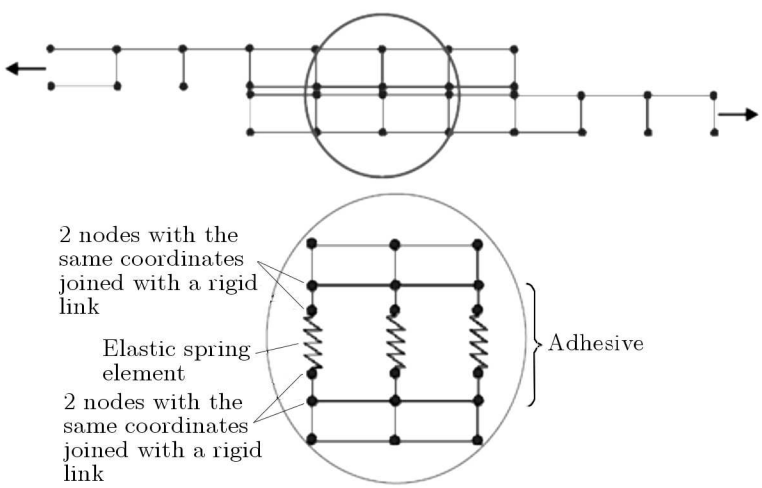

Fig. 5. Finite element modeling of the adhesive zone (Trias *et al.*, 2006)

In the case of FE mathematical modelling, a mesh encompassing the structure is generated. The stiffness matrix of each element and the structure is determined. The loads applied to the structure are replaced by an equivalent force system such that the forces act at the nodal points. According to the basic FE formulation, it can be written

$$\mathbf{K}\boldsymbol{u} = \boldsymbol{F} \tag{4.1}$$

where $\mathbf{K}$ and $\boldsymbol{u}$ represent the element stiffness matrix and the displacement vector. The displacements at a point inside the element are calculated by

$$\boldsymbol{u} = \mathbf{N}\boldsymbol{\delta} \tag{4.2}$$

where $\mathbf{N}$ is the matrix of the shape vectors. The strains at a point inside the elements are calculated by

$$\boldsymbol{\varepsilon} = \mathbf{B}\boldsymbol{\delta} \tag{4.3}$$

where, $\mathbf{B}$ is the strain-displacement matrix. The elastic behaviour is written in terms of an elastic constitutive matrix that relates the nominal stresses to the nominal strains across the interface. The corresponding nominal strains can be defined as

$$\varepsilon_n = \frac{\delta_n}{\tau_0} \qquad \varepsilon_s = \frac{\delta_s}{\tau_0} \qquad \varepsilon_t = \frac{\delta_t}{\tau_0} \tag{4.4}$$

where $\boldsymbol{\tau}$ and $\boldsymbol{\delta}$ denote the nominal traction stress vector and displacement fields, respectively, while the parameters with the subscript n, s and t represent the nominal, shear and the area between the top and bottom of the cohesive layer, respectively. The stresses at a point inside the element are calculated by

$$\boldsymbol{\sigma} = \mathbf{E}\boldsymbol{\varepsilon} \tag{4.5}$$

where $\mathbf{E}$ is the stiffness matrix characterising the composite material. The element stiffness matrix is

$$\mathbf{K} = \int_V \mathbf{B}^\top \mathbf{E}\mathbf{B}\, dV \tag{4.6}$$

where V is the volume of the element.

The cohesive element formed by 4 nodes $(n = 2)$ can be used to connect continuum plane strain elements with two degrees of freedom per node. The cohesive element formed by 8 nodes $(n = 3)$ can be used to connect three-dimensional continuum elements with three degrees of freedom per node. The

constitutive equations of the cohesive element relate the tractions τ_i at the midsurface of the element to the displacement jumps Δ_m. The contribution of the element to the tangent stiffness matrix and to the residual vector, i.e., the internal force vector of the cohesive element can be shown

$$f_{Ki} = \int_{\Gamma_{d_i}} \tau_i B_{imK} \, d\Gamma_d \tag{4.7}$$

where

$$B_{imK} = \Theta_{im} \overline{N}_K \tag{4.8}$$

The rotation tensor Θ_{im} relates the global and the local coordinates. The softening nature of the cohesive element constitutive equation causes difficulties in obtaining a converged solution to the non-linear problem when using the Newton-Raphson iterative method. The Newton-Raphson method is based on Taylor's series expansion of a set of nonlinear algebraic equations. The equations must be solved using an iterative method. To formulate the equations to be solved at the $(n+1)$-st iteration by the Newton-Raphson method, it is assumed that the solution at the n-th iteration is known. In particular, quadratic convergence is not assured because the residual vector is not continuously differentiable with respect to the nodal displacements. The tangent stiffness matrix stems from the linearization of the internal force vector and it is obtained using Taylor's series expansion. Taking into account that the calculation of the geometric terms of the tangent stiffness matrix is computationally very intensive, these terms are neglected. The tangent stiffness matrix, K_{rzik}, for the cohesive element is therefore approximated as

$$K_{jkrz} \approx \int_{\Gamma_d} B_{ijk} D_{in}^{tan} B_{nrz} \, d\Gamma_d \tag{4.9}$$

where D_{in}^{tan} is the material tangent stiffness matrix, or a constitutive tangent tensor used to define the tangent stiffness matrix. It depends on the interfacial constitutive model adopted. The process of degradation begins when the stresses and/or strains satisfy certain damage initiation criteria. Damage is assumed to initiate when the maximum nominal stress ratio reaches a value of one. This criterion can be expreseed as in equation (4.10)

$$\max\left\{\frac{T_n}{T_n^0}, \frac{T_s}{T_s^0}, \frac{T_t}{T_t^0}\right\} = 1 \tag{4.10}$$

where T_n^0, T_s^0 and T_t^0 represent the peak values of the nominal stress when the deformation is either purely normal to the interface or purely in the first

or second shear direction, respectively. The symbol $\left\langle \cdot \right\rangle$ used represents the Macaulay bracket with the usual interpretation. The Macaulay brackets are used to signify that a pure compressive deformation or stress state do not initiate damage.

5. Material properties

The material properties of each layer of fiberglass 200 g/m^2 are obtained from the material characterisation test data that was cited by Dahdi *et al.* (2009). The summary of mechanical properties of C-glass/epoxy 200 g/m^2 is shown in Table 2.

Table 2. Mechanical properties of C-glass/epoxy 200 g/m^2 (Dahdi *et al.*, 2009)

Properties	C-glass/Epoxy 200 g/m^2
E_{11}	3.5 GPa
E_{22}	3.5 Gpa
ν_{12}	0.158
G_{12}	2.340 Gpa
G_{13}	2.340 Gpa
G_{23}	2.340 Gpa

For many material systems, the fracture toughness can be measured experimentally; however, the value of separation at the final failure as well as the shape of the softening portion of the traction-separation relation may be difficult, if not impossible, to determine. Thus, it is easier to use an energy-based damage evolution with linear softening behaviour. The adhesive bond between the layers is modelled using the cohesive element functionality via ABAQUS (Lapczyk and Hurtado, 2007). A triangular traction-separation cohesive law with linear softening is used to represent the mechanical response of the cohesive element. Adhesive epoxy material properties in Table 3 are also used in the proposed model (Lapczyk and Hurtado, 2007).

Herein, K_n, K_s, and K_t are the initial interface stiffnesses, and T_n^o, T_s^o and T_t^o are the interface strengths. G_{IC}, G_{IIC} and G_{IIIC} also define the interface fracture toughness and the modal dependence of damage evolution. The parameters coming with the subscript n, s and t represent the material properties at the normal mode, first and second shear direction, respectively.

Table 3. Summary of mechanical properties of adhesive epoxy (Lapczyk and Hurtado, 2007)

Properties	Adhesive epoxy
K_n	2000 MPa
K_s	2000 MPa
K_t	2000 Mpa
T_n^o	50 MPa
T_s^o	50 MPa
T_t^o	50 MPa
G_{IC}	4 N/mm
G_{IIC}	4 N/mm
G_{IIIC}	4 N/mm
ν	0.33

6. Results and disscussion

FEA results of the fuselage model with the cohesive elements obtained using ABAQUS/Explicit for the deformation modes, and load-displacement are shown in Figs. 6 and 7.

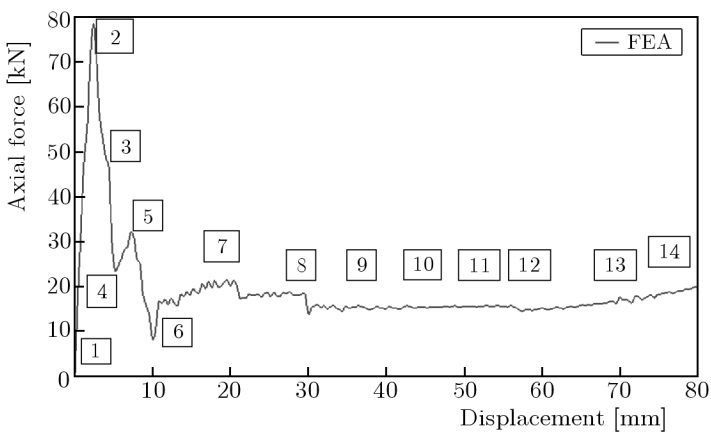

Fig. 6. Load-displacement vs. axial force

It can be seen that in Fig. 6, at the beginning of the loading operation, the applied load rises linearly up to point 2, where the load maximum is obtained. The maximum recorded load at point 2 was 78 kN at 2.4 mm displacement. In the next step, the load-displacement curve drops off suddenly to point 4.

During compression of 5.2 mm at point 4, debonding was observed between the fuselage sections. Figure 7 clearly shows the collapse modes at each stage.

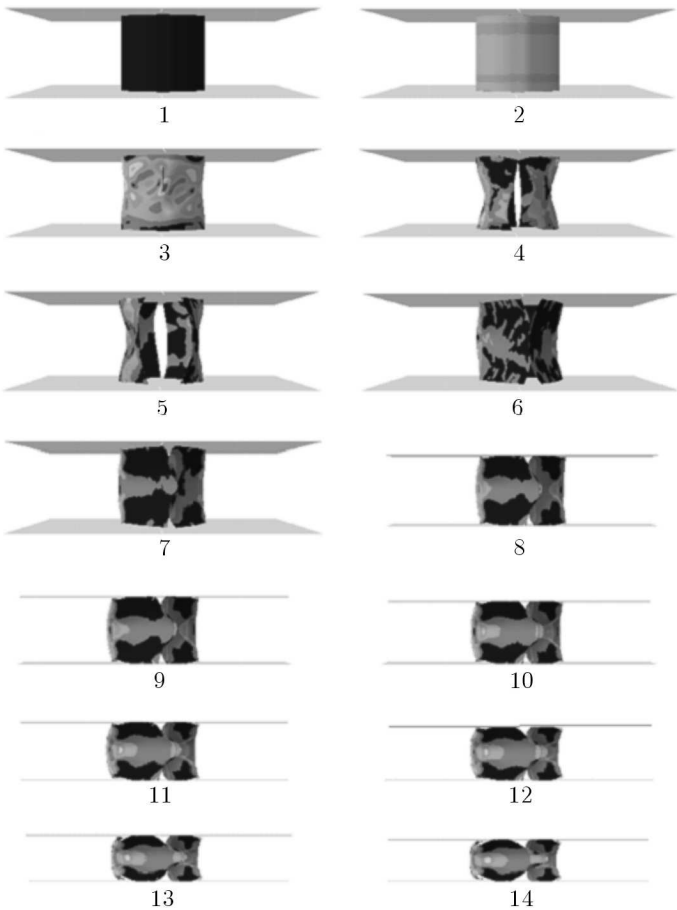

Fig. 7. Collapse modes from FEA model

7. Verification of FEA modelling

It can be concluded that there is a good agreement between the experimental and FEA results throughout the loading process (Fig. 8). The tendency through the crushing loading for both experiment and simulation is very close. Clearly, the applied load at the start of the loading process increases linearly up to the point where the load maximum is reached. It can be seen that after the maximum loading step, the experimental and the numerical load-displacement curves drop off sharply at nearly the same displacement.

From the visual comparison of the peak load value achieved by the experiment and the numerical analysis in Table 4, the peak load for the experiment specimen is 77 kN and 78 kN for the numerical results. One-percent error is estimated for the peak load between the experiment and the failure theories used to simulate the progressive damage (see Table 4). According to Figs. 8 and 9, the collapse modes and crushing behaviour for both the experiment and simulation are found correlated.

Table 4. Peak load deviation [%] between FEA and experimental results

Test	Peak load [kN]	Displacement [mm]
FEA simulation	78	2.4
Experiment test	77	3.79
Discrepancy [%]	1	39

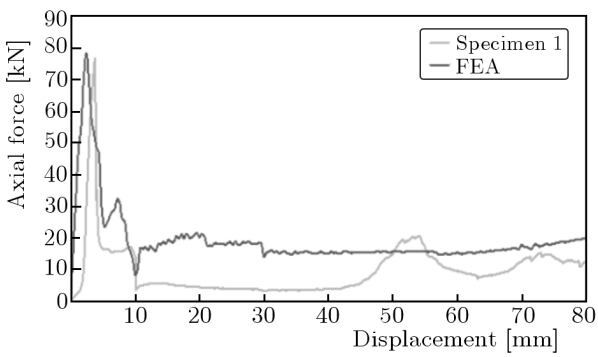

Fig. 8. Load-displacement vs. axial force for comparing experimental and FEA results

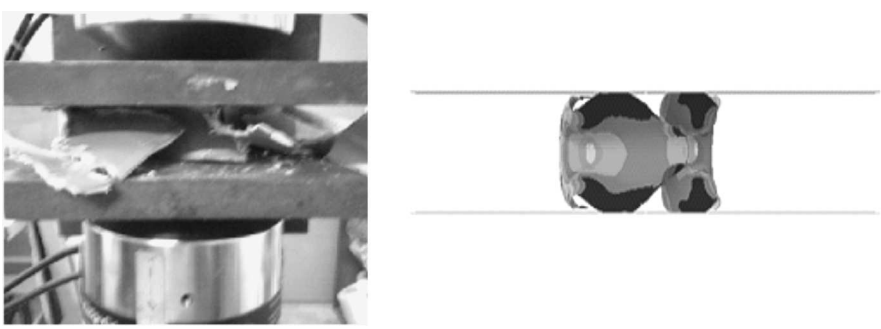

Fig. 9. Collapse modes for experimental test vs. FEA results

8. Parametric study

The finite element results show a good agreement with the experimental ones, and give confidence in replacing very time consuming actual quasi-static tests with computer simulations. After confirmation of numerical analysis by an experimental study, the effect of the angle of orientation and special cases of laminates on the crushing behaviour of a C-glass/epoxy fuselage section by FEA can be discussed and presented.

To obtain and visualize the effects of each angle orientation of the lamina, various angles of the lamina are deliberated. As can be seen from Table 5, fuselage sections that are modelled in this study consisted of 8 plies of C-Glass/Epoxy 200 g/m^2 in the special cases of laminates (Bisagni, 2005). Symmetric, cross-ply, angle-ply, antisymmetric, balanced and quasi-isotropic laminates are all types of lamina models that are examined in this research.

Table 5. Special cases of laminates

Laminate	Orientation	Abbreviation
Antisymmetric	$[45_4/\text{-}45_4]$	Antisym
Angle-ply symmetric	$[\text{-}45/45/\text{-}45/45]_s$	APLSym
Angle-ply	[-45/45/-45/45/-45/45/-45/45]	APL
Cross-ply symmetric	$[0/90/0/90]_s$	CPLSym
Cross-ply	[0/90/0/90/0/90/0/90]	CPL
Balanced	[45/-45/-45/45/-45/-45/45/45]	BalL
Quasi-isotropic	$[45/\text{-}45/90/0]_s$	QuaIso

The results obtained from the load-displacement response for the special cases of laminates are shown in Figs. 10 and 11 and Table 6, when they are applied to the fuselage sections. It is apparent from these figures that there are two patterns of load-displacement curves, namely the pattern X (i.e. CPLSym with CPL) and Y (i.e. Antisym, APLSym, APL, BalL with QuaIso). The pattern X seems to have more resistance to the applied load than Y. The most striking result emerging from FEA is more or less the same amount of peak load for laminates Antisym, APLSym, APL and BalL namely 90 kN (Table 6). As can be seen from Table 6, CPLSym and CPL laminates seem to have approximately the same amount of peak load, 78-80 kN. Further analysis showed that QuaIso laminated peak load goes down between the two groups that are 85 kN. This study confirmed that both patterns more or less maintain constant loads after reaching the lowest load and fail at an approximately 2.4 mm displacement. It can be said that CPLSym and CPL were found giving similar trends to the baseline model of $[90_8]$.

Table 6. Baseline and special cases comparison for the peak load and displacement of laminates

Test	Peak load [kN]	Displacement [mm]
Baseline	78	2.4
Antisymmetric	91	2.4
Angle-ply symmetric	90	2.4
Angle-ply	90	2.4
Cross-ply symmetric	80	2.4
Cross-ply	78	2.4
Balanced	90	2.4
Quasi-isotropic	85	2.4

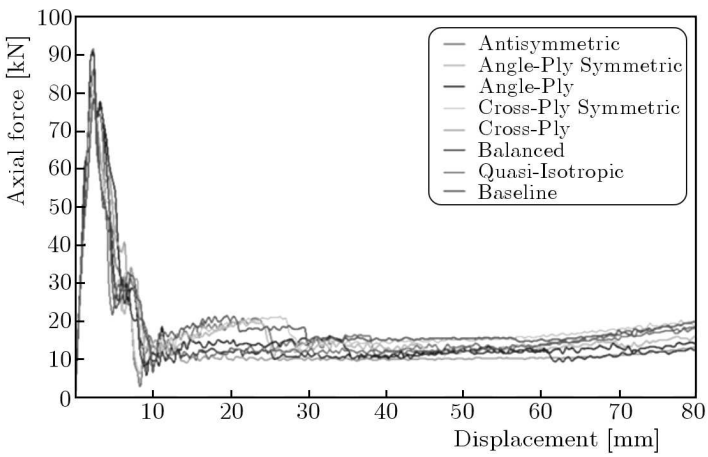

Fig. 10. FEA load-displacement curve of special laminates

9. Conclusion

In this research, FEA simulation of a fuselage structure under axial compression loading is investigated to predict the crushing behaviour and mechanical strength. A woven C-glass fiber/epoxy 200 g/m^2 composite laminated with orthotropic elastic material properties is modelled by employing ABAQUS/Explicit. Various angles of the lamina are considered in the analysis to obtain the effect of the angle of orientation. The following summary may be drawn:

- Finite element analysis using ABAQUS/Explicit can reproduce acceptable load-deflection responses compared with the experimental works.

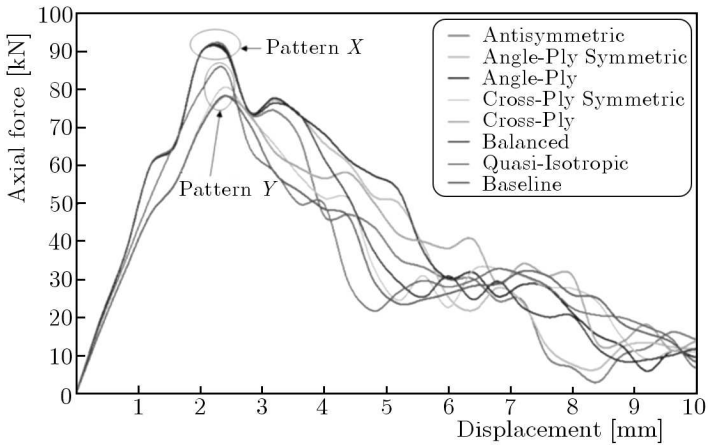

Fig. 11. FEA load-displacement curve of special laminates (Enlarged)

- Finite element simulation results concerning the main crushing characteristics such as the peak load and crush energy absorption are very close to the experimental results.
- Using ABAQUS/Explicit, a reliable FEA model to predict the adhesive joint of composite fuselage structure was successfully developed.
- The adhesive joint was successfully modelled utilizing the cohesive elements to predict the adhesive behaviour and strength.
- The validated FEA model was also applied for parametric study, and was used to provide a good insight on how the ply orientation affects the structure strength.
- It can be suggested that antisymmetric lamination is found to have the most resistance to the applied load.

Acknowledgment

This research was supported by Fundamental Research Grant Scheme (FRGS5524003).

References

1. BALZANI C., WAGNER W., 2008, An interface element for the simulation of delamination in unidirectional fiber-reinforced composite laminates, *Engineering Fracture Mechanics*, **75**, 9, 2597-2615
2. BISAGNI C., 2005, Dynamic buckling of fiber composite shells under impulsive axial compression, *Thin-Walled Structures*, **43**, 3, 499-514

3. CHAMIS C.C., ABUMERI G.H., 2005, Probabilistic dynamic buckling of composite shell structures, *Composites Part A: Applied Science and Manufacturing*, **36**, 10, 1368-1380

4. DAHDI I., EDI Y., MUSTAPHA F., ZAHARI R., 2009, Novel fabrication for tubular and frusto conical composite product for aerospace application, *Conferences Proceeding of Aerotech III*

5. GOYAL V.K., JOHNSON E.R., 2008, Predictive strength-fracture model for composite bonded joints, *Composite Structures*, **82**, 3, 434-446

6. KOUSSIOS S., BERGSMA O., BEUKERS A., 2004, Filament winding. Part 1: Determination of the wound body related parameters, *Composites Part A: Applied Science and Manufacturing*, **35**, 2, 181-195

7. LAPCZYK I., HURTADO J.A., 2007, Progressive damage modeling in fiber-reinforced materials, *Composites Part A: Applied Science and Manufacturing*, **38**, 11, 2333-2341

8. MAHDI E., MOKHTAR A., ASARI N., ELFAKI F., ABDULLAH E., 2006, Nonlinear finite element analysis of axially crushed cotton fibre composite corrugated tubes, *Composite Structures*, **75**, 1/4, 39-48

9. MAHDI E., SAHARI B., HAMOUDA A., KHALID Y., 2001, An experimental investigation into crushing behaviour of filament-wound laminated cone-cone intersection composite shell, *Composite Structures*, **51**, 3, 211-219

10. MAMALIS A., MANOLAKOS D., IOANNIDIS M., PAPAPOSTOLOU D., 2006, The static and dynamic axial collapse of CFRP square tubes: finite element modelling, *Composite Structures*, **74**, 2, 213-225

11. MORTHORST M., HORST P., 2006, Crushing of conical composites shells: a numerical analysis of the governing factors, *Aerospace Science and Technology*, **10**, 2, 127-135

12. TAFRESHI A., 2004, Efficient modelling of delamination buckling in composite cylindrical shells under axial compression, *Composite Structures*, **64**, 3/4, 511-520

13. TAFRESHI A., 2006, Delamination buckling and postbuckling in composite cylindrical shells under combined axial compression and external pressure, *Composite Structures*, **72**, 4, 401-418

14. TARFAOUI M., GNING P., HAMITOUCHE L., 2008, Dynamic response and damage modeling of glass/epoxy tubular structures: Numerical investigation, *Composites Part A: Applied Science and Manufacturing*, **39**, 1, 1-12

15. TRIAS D., ROJO R., NUIN I., LASA M., 2006, Fracture mechanics and new techniques and criteria for the design of structural components for wind turbines, Technical paper presented at EWEC06.

16. VAZIRI A., 2007, On the buckling of cracked composite cylindrical shells under axial compression, *Composite Structures*, **80**, 1, 152-158

17. WIMMER G., SCHUECKER C., PETTERMANN H., 2006, Numerical simulation of delamination onset and growth in laminated composites, *The e-Journal of Nondestructive Testing*, **11**, 1-10
18. XIAO X., MCGREGOR C., VAZIRI R., POURSARTIP A., 2009, Progress in braided composite tube crush simulation, *International Journal of Impact Engineering*, **36**, 5, 711-719
19. YANG Z., SU X., CHEN J., LIU G., 2009, Monte Carlo simulation of complex cohesive fracture in random heterogeneous quasi-brittle materials, *International Journal of Solids and Structures*, **46**, 17, 3222-3234
20. YIDRIS H.N., MOKHTAR A.M., 2007, *Crush Simulation and Experimental Validation of a Composite Unmmaned Aerial Vehicle Fuselage Section*, Universiti Putra Malaysia, pp. 161
21. ZAREI H., KROEGER M., ALBERTSEN H., 2008, An experimental and numerical crashworthiness investigation of thermoplastic composite crash boxes, *Composite Structures*, **85**, 3, 245-257
22. ZHANG Z., CHEN H., YE L., 2008, Progressive failure analysis for advanced grid stiffened composite plates/shells, *Composite Structures*, **86**, 1/3, 45-54

Badania przebiegu osiowego zgniatania modelu kompozytowego kadłuba z wykorzystaniem elementów kohezyjnych

Streszczenie

Pracę poświęcono analizie elementów skończonych w zastosowaniu do badań modelu miniaturowego kadłuba wykonanego z laminatu i poddanego osiowemu ściskaniu. Przeprowadzono symulacje numeryczne z użyciem komercyjnego oprogramowania ABAQUS/Explicit w celu określenia wytrzymałości kompozytu oraz zbadania przebiegu procesu zgniatania, aż do uzyskania ostatecznej postaci zniszczenia próbki. Na materiał kadłuba wybrano kompozyt w włóknem szklanym typu C o gęstości $200\,\mathrm{g/m^2}$ i właściwościach ortotropowych. Podczas badań obserwowano pojawianie się kolejnych postaci wgnieceń, aż do zupełnej utraty stateczności układu przy udarowym obciążeniu ściskającym. Zastosowano metodę elementów kohezyjnych do analizy zmian w adhezyjnym połączeniu warstw laminatu. Zbadano wpływ kąta laminowania na właściwości próbki. Przeprowadzono także badania parametryczne wpływu kąta laminowania modelu metodą elementów skończonych. Uzyskane wyniki wykazały, że symulacje wykonane w systemie ABAQUS/Explicit wiarygodnie odtwarzają rzeczywisty przebieg zgniatania w funkcji przykładanego obciążenia. Zaobserwowano również, że niektóre przypadki laminowania antysymetrycznego są szczególnie odporne na zniszczenie wywołane siłą osiową.

Manuscript received July 18, 2011; accepted for print October 7, 2011